Technical Paper

ISSN 1997-1400 Int. J. Pavement Res. Technol. 6(6):755-764

Evaluation of Pavement Layer Moduli using Instrumentation Measurements

Xiaochao Tang[1+], Shelley M. Stoffels[2], and Angelica M. Palomino[3]

Abstract: Instrumentation embedded in pavements is increasingly being used to measure the critical responses and monitor performance of specially-constructed experimental pavement sections or in-service pavements under controlled wheel loading or live traffic. On the other hand, nondestructive tests (NDT), such as falling weight deflectometer (FWD) testing, are routinely performed to evaluate pavement layer structural properties based on deflections measured on the surface of the pavements. In cases where measurements from the pavement surface only are not sufficient to infer pavement layer modulus values, e.g. rolling wheel deflectometer (RWD) tests typically with only one deflection measurement or complex geometries, a procedure that combines measurements from the embedded instruments and surface deflections would provide an alternative to the traditional backcalculation of pavement layer moduli. This study presents an inverse analysis procedure integrating finite element (FE) models and a population-based optimization technique, Covariance Matrix Adaptation Evolution Strategy (CMA-ES), to determine the pavement layer structural properties. Tests using a lightweight deflectometer (LWD) were conducted on instrumented three-layer scaled flexible pavement test sections. The time histories of the LWD load, surface deflection underneath the LWD load, subgrade deflection and vertical stress were recorded and used in the inverse analysis. While the common practice in backcalculating pavement layer properties still assumes a static FWD load and makes use of only peak values of the load and deflections, dynamic analysis was conducted to simulate the impulse LWD load. Results of the inverse analysis show that consistent pavement layer properties can be obtained based on the LWD surface deflection data and measurements of the embedded instrumentation.

DOI: 10.6135/ijprt.org.tw/2013.6(6).755
***Key words**: Evolution strategy; Finite element; Inverse analysis; Optimization; Pavement instrumentation.*

Introduction

Over the decades, instrumentation technology has been increasingly adopted to measure critical responses of pavements to traffic load and monitor the performance of pavements [1-6]. Along with the release of the mechanistic-empirical (ME) pavement design program, DARWin-ME by AASHTO, the need for model calibration and verification will continue to expand [7, 8]. A number of recent studies aimed at refining the ME models and aiding in the implementation of MEPDG have used a variety of embedded instruments to monitor the long-term behavior of in-service pavements [9-11]. The future instrumentation of pavements as a component of structural health and response monitoring systems is also being seriously explored, and is increasingly seen as viable [12, 13]. Since embedding instrumentation in pavements is perhaps the most reliable way to measure the in-situ pavement responses and performance, the application of instrumentation in pavements is expected to continue growing.

Backcalculation of flexible pavement layer properties based on falling weight deflectometer (FWD) testing has been routinely used as a tool for evaluating the structural capacities of pavements. Traditional backcalculation of pavement layer moduli involves using the measured surface deflection basin data, i.e. peak pavement surface deflections measured at the location underneath the impulse load of an FWD and locations with certain offsets from the load [14, 15]. The FWD backcalculation of pavement layer properties is essentially an inverse problem with known input signals into a system and known output signals based on which unknown system parameters are identified [16]. It is therefore possible to backcalculate pavement layers' properties from any known loads applied to the pavement and any properly measured pavement responses. The load applied to the pavement can be the impulse FWD load or rolling wheel load while pavement responses include surface deflections and measurements from instruments embedded in the pavement system.

There are cases where measurements from the pavement surface only are not sufficient to infer pavement modulus, e.g. rolling wheel deflectometer (RWD) tests typically with only one deflection measurement or complex pavement geometries, which would lead to an indeterminate problem with non-unique solutions. The inverse analysis procedure combining measurements from the embedded instruments and measurements on the surface would provide an alternative to the traditional backcalculation of pavement layer moduli. Furthermore, as the strategic objective of highway renewal research in the second Strategic Highway Research Program (SHRP 2) is to develop the necessary tools to "get in, get out, and stay out" when renewing highway pavements, the increasingly widespread use of pavement instrumentation in in-service pavements provides

[1] Department of Civil Engineering, Widener University, One University Place, Chester, PA 19013 USA.
[2] Department of Civil and Environmental Engineering, Pennsylvania State University, 208 Sackett Building, University Park, PA 16803, USA.
[3] Department of Civil and Environmental Engineering, University of Tennessee, 73E Perkins Hall, Knoxville, TN 37996, USA.
[+] Corresponding Author: E-mail xtang@widener.edu
Note: Submitted December 30, 2012; Revised April 4, 2013; Accepted April 9, 2013.

the potential to evaluate and monitor the in-situ structural properties of in-service pavements with significant less interruption of traffic and compromise of safety at the tested sites [17]. To demonstrate the inverse analysis procedure based on instrumentation measurements, this study presents using a lightweight deflectometer (LWD) to infer the moduli of an instrumented three-layer scaled flexible pavement test section. Inverse analysis based on site-specific finite element (FE) forward modeling was conducted to backcalculate the pavement layer properties using the information of the recorded LWD data and measurements of the deflection and vertical stress at the top of the subgrade from instrumentation.

Instrumented Test Section

Test Section

Two sets of test sections were constructed in a pit bounded by reinforced concrete walls. The pavement section within the pit was 206 cm (81 in) long, 91 cm (36 in) wide, and 127 cm (50 in) deep. The pavement test sections were constructed in the pit on top of a densely compacted 2.5-m layer of AASHTO No. 57 aggregate. The scaled pavement was a three-layer flexible pavement structure: a 4-cm asphalt layer, a 10-cm aggregate base course, and a 113-cm soil subgrade layer as shown in Fig. 1. The two sets of flexible pavement test sections were built with the same dimensions and pavement materials except for the subgrade soil types and subgrade conditions.

Studies were carried out to investigate possible boundary effects due to both the side walls and backfill aggregate foundation underlying the soil subgrade. The investigation focused on the impact of various boundaries on a critical pavement response, namely vertical stresses at the top of the subgrade. A previous study was conducted on an unpaved aggregate-subgrade structure to investigate the effects of subgrade thickness on the pavement critical responses. Results showed that the change of vertical stress atop subgrade becomes minimal when the subgrade thickness is about 100 cm (40 inches). Therefore, it is assumed that the 113-cm (44.5 inches) thick subgrade for the proposed pavement cross section with the addition of an asphalt layer has negligible boundary effects due to the backfill underlying the subgrade. A series of linear static two-dimensional axisymmetric finite element (FE) models with different radial distances between the load center and the radial boundary were created to study the effects of side walls on the pavement responses. The study showed that the 46 cm distance between the center and the nearest boundary has insignificant effects on the change of vertical stresses at the top of subgrade.

The asphalt layer was constructed using a 9.5-mm surface mix containing a PG 64-22 binder. No dynamic modulus tests were conducted to characterize the stiffness of the asphalt mixture. The base layer was constructed using a dense-graded crushed limestone. Two different types of soil designated as Soil 1 and Soil 2 were used as pavement subgrades. They are classified as lean clay with sand (CL) and silt with sand (ML) or A-4(5) and A-4(4) for Soil 1 and Soil 2, respectively. The percentage passing the #200 sieve (0.075 mm) for Soil 1 and Soil 2 are 77.6 and 83.2 and plasticity indices are 8.1 and 4.4, respectively. The optimal moisture contents for Soil 1 and Soil 2 are 18% and 19% and maximum dry densities are 1700

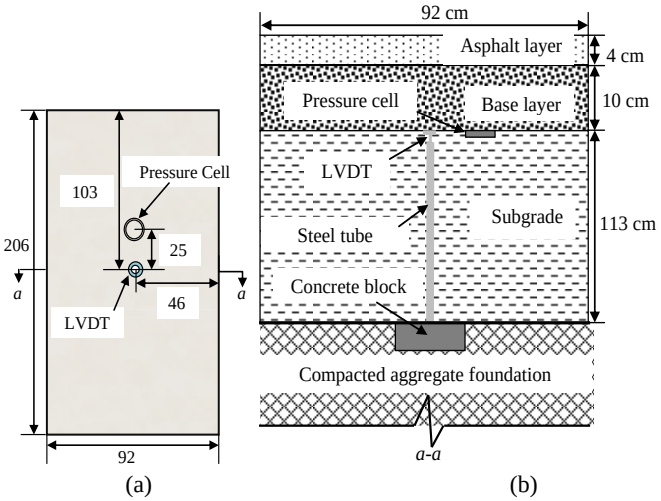

Fig. 1. Schematic and Dimensions of a Typical Test Section: (a) Plan View of the Test Section; Cross Section of the Section and Position of the LVDT.

kg/m^3 and 1690 kg/m^3, respectively. During construction, the soil was compacted at a water content greater than optimum to induce soft subgrade conditions. The subgrade CBR was maintained at 2.0 and 1.5 for the two individual sets of tests based on the relationship between CBR and water content developed through a series of CBR tests.

Instrumentation

The elastic deflection at the subgrade was recorded by using linear variable differential transformers (LVDTs) (Macro Sensors GHSE-750-1000). The maximum travel distance of the push rod is 25.4 mm (1 in). The overall length of the LVDT is 29 cm (11.4 in). The linearity error of the LVDT is less than 0.06% and the repeatability error is less than 0.6 μm.

The installation of each LVDT was accomplished in two steps. Prior to the construction of subgrade, a steel tube for housing the LVDT was mounted on a concrete slab and placed at the center of the test section as shown in Fig. 1. The concrete slab was leveled as much as possible to ensure the horizontal level of the subsequent LVDT installation (Fig. 2(a)). The cable for the LVDT was also protected from angular aggregate particles by using a PVC pipe. After the construction of subgrade, the LVDT was connected to the cable and inserted into the steel tube by excavating the built subgrade to avoid possible damage to the LVDT during the subgrade construction. A thin yet rigid disk with diameter of 5 cm (2 in) was attached onto the contact tip of the spring-loaded LVDT to provide sufficient contact area. The contact tip was wrapped with thin, flexible membrane to avoid the intrusion of soil particles into the LVDT. The LVDT was totally immersed in the soil with its contact disk flush with the soil surface. The LVDT measured the total deflection of the subgrade, since the end of each LVDT was fixed with respect to the bottom of the subgrade.

The vertical stress at the top of the subgrade was measured using a hydraulic type earth pressure cell with semiconductor transducer (Geokon 3500) and a diameter of 10.2 cm (4.0 in). The pressure cell has a full-scale range of 250 kPa (36.3 psi), which can provide

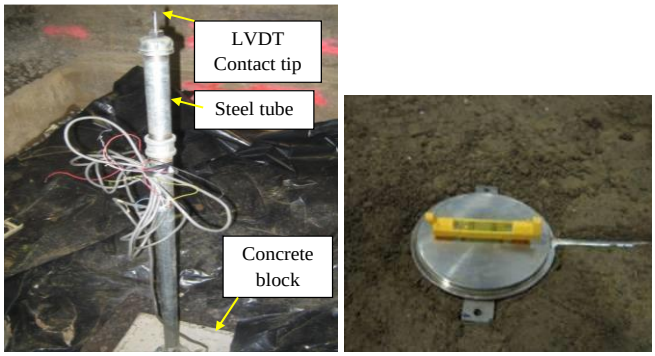

(a) (b)

Fig. 2. Instrumentation Used in this Study: (a) a LVDT was Housed in a Steel Tube Mounted on a Concrete Slab; (b) Earth Pressure Cell was Leveled before Being Covered by Soil.

satisfying resolution and range since the pressure was expected to be about 20 kPa (3 psi) in this application. The pressure cell has the following specifications: ±0.5% calibrated accuracy, < 0.05% thermal effect on zero, < 0.5% linearity.

The pressure cell was installed at the location about 25 cm (10 in) from the center of the section upon the completion of the subgrade layer construction (Fig. 1). The subgrade was excavated using small hand tools for placement of the pressure cell. The pressure cell was installed about 1.3 cm (0.5 in) below the subgrade surface. Care was taken to ensure that the pressure cell was positioned and leveled (Fig. 2(b)). Details on the installation of the instruments used in this study can be found elsewhere [18].

LWD Testing

A portable light weight deflectometer (Carl BroTM PRIMA 100) was used for assessment of in situ pavement layer moduli. By dropping a weight with a mass of 10 kg from a certain height, the LWD applies an impulse load to the pavement through the bearing plate with a diameter of 30 cm. The impulse load was measured using a load cell, and the surface deflections were measured with accelerometer. The main purpose of the LWD tests was to measure the pavement responses (surface deflections) to a known load and to use the measurements to backcalculate the resilient modulus of each of the pavement layers.

LWD tests were conducted on each pavement layer as the construction progressed. The LWD was not able to yield meaningful measurements when testing directly on both of the soil subgrades because the subgrades were too weak to experience resilient deflection under the LWD load. In order to adjust the LWD impulse load to accommodate the deflection measurement, the LWD weight was dropped at the height of 0.61 m for LWD tests on the base layer and 0.91 m for LWD tests on the asphalt layer, which generates a peak load of about 4.8 kN and 9.2 kN, a peak stress of 65.0 kPa and 130.0 kPa, respectively. It is noted that the load applied on the pavement is lower than the standard full-scale axle load due to the limitation of LWD's light weight. However, for the purpose of backcalculating the pavement layer moduli, the loading level of the LWD on the scaled pavement test sections is sufficient, which is proved by the measurements from the LVDT and pressure cell at the top of the subgrade. LWD tests were performed for each section on the base layer and asphalt concrete layer at locations above the LVDT and pressure cell. The responses from the LVDT and pressure cell to the LWD loading were recorded. The time histories of the LWD load and the surface deflection underneath the loading plate were also recorded and used in the subsequent dynamic linear backcalculation procedure.

Forward Modeling

Geometric Model and Material Properties

The backcalculation of the properties of flexible pavement layers is a parameter identification problem involving two primary components: (1) the forward modeling of the pavement system and (2) the inverse analysis based on measurements. In this study, finite element (FE) modeling was adopted to serve as the forward model. While it is ideal to use a three-dimensional FE model to simulate the actual geometries of the pavement test sections, a three-dimensional model demands much more computational resources due to the increased number of elements. The cost of computational time and resources was considered when creating the FE models because the FE model will be called repeatedly during the inverse analysis.

The test section was simplified as an axisymmetric model since the LWD load can be approximated as a uniformly-distributed circular load and is axially symmetric. The axisymmetric model is less computational resource-demanding than a 3-dimensional model. The general-purpose FE package, ABAQUS® , was used to create the 2-dimensional axisymmetric model. Fig. 3(a) shows the plan view of one test section. The problem is symmetric with respect to the axis passing through the center of the loaded area up to the nearest boundary with a radial distance of 46 cm. Through the axisymmetric model, the rectangular block is now reduced to a cylinder - the circle in Fig. 3(a) extruding into the plane of the page to the depth of the pavement. The FE model of the pavement test section uses first-order quadrilateral solid elements (CAX4R). The element has four nodes and a total of eight degrees of freedom with each node, having two degrees of freedom in the vertical and radial directions. Non-uniform meshes were used in discretizing the model. Finer meshes were assigned at the regions closer to the load and of greater interests (Fig. 3(b)). The FE model consists of 12,150 nodes and 11,920 elements.

Boundaries were assigned to both the outer perimeter and the rotation axis, as well as the bottom of the model. It should be pointed out that boundaries were added to the symmetry axis in the FE model, although the axis physically is the central line of the cylinder and does not have boundaries. The nodes on the rotation axis and outer perimeter were restrained in the radial direction but allowed to move in the vertical direction. The nodes at the bottom of the model were restrained in the vertical direction.

In this study, the pavement materials were assumed to be linear elastic although they may have nonlinear behavior, e.g. stress-dependence for base aggregates and time-dependency for the asphalt concrete. Elastic modulus and Poisson's ratio were the only material inputs for the static analysis, and a Rayleigh damping ratio was assigned to each pavement layer during the dynamic analysis. Poisson's ratios for the asphalt concrete, aggregate base, and soil subgrade were assumed to be 0.30, 0.35, and 0.45, respectively [19].

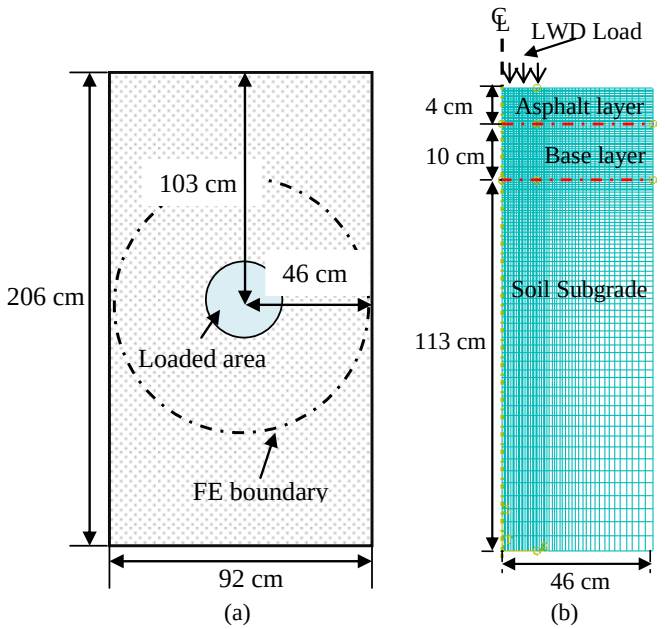

Fig. 3. Geometries and Mesh of the Axisymmetric Finite Element Model for the Test Section: (a) Plan View of the Test Section with the Circular Area Representing the FE Geometric Model; (b) Cross-section View of the FE model, Not to Scale.

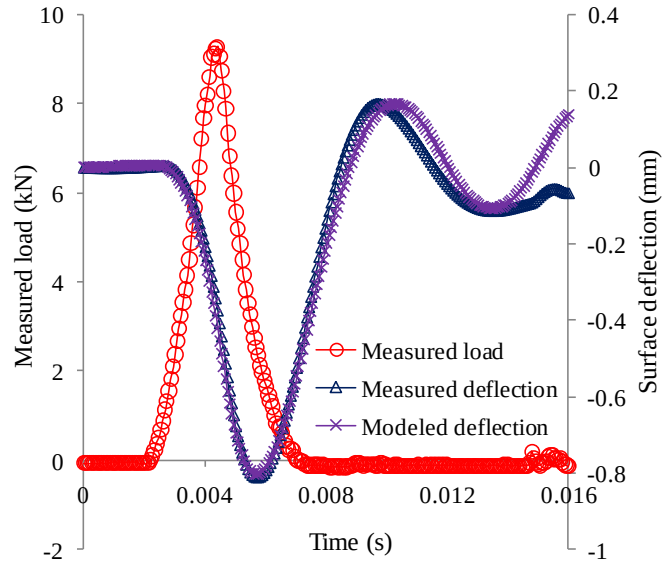

Fig. 4. Time Histories of the Measured LWD Load, Measured Central Surface Deflection, and Modeled Central Surface Deflection.

Dynamic Analysis of LWD Load

Fig. 4 shows the recorded time histories of the LWD load and the surface deflection underneath the LWD load plate. The time lag between the load and deflection indicates the inertial and damping effects and the dynamic nature of the impulse LWD load. Thus, a dynamic analysis of a LWD test would be more realistic than a static analysis. However, due to the complexity of dynamic analysis and its high computational cost, static analysis has been traditionally adopted in the practice of backcalculating pavement layers' properties. For the purpose of comparison, both the static and dynamic analysis of LWD tests was conducted in this study. While the measured peak value of the LWD load was used for the static analysis, the collected load-time history data were used for the dynamic analysis.

The LWD test can be simplified as a single degree of freedom (SDOF) system subjected to an external dynamic load, in this case the LWD impulse load as a function of time. The equation of motion for the SDOF system with known mass, stiffness, and damping can be expressed as follows [20]:

$$M\ddot{U} + C\dot{U} + KU = F(t) \tag{1}$$

in which M is the mass of the SDOF system; C is the damping coefficient; K is stiffness; U, $\dot{U}$, $\ddot{U}$ are displacement, velocity, and acceleration, respectively; $F(t)$ is the external load as a function of time measured with the load cell of the LWD.

The recorded time-history of the impulse LWD load was incorporated into the FE model of the pavement section. The dynamic equilibrium equation discussed above for the pavement system subjected to the LWD load was solved through time integration based on the central difference integration rule using ABAQUS® /Explicit. The mid-increment value of velocity is determined from the known velocity, $\dot{U}_{(t-\Delta t/2)}$ and acceleration, $\ddot{U}_t$ from the previous increment:

$$\dot{U}_{(t+\Delta t/2)} = \dot{U}_{(t-\Delta t/2)} + \frac{\Delta t^{(t+\Delta t)} + \Delta t^{t}}{2}\ \ddot{U}_t \tag{2}$$

The displacement at the end of the increment is calculated as follows:

$$U_{(t+\Delta t)} = U_t + \Delta t^{(t+\Delta t)}\ \dot{U}_{(t+\Delta t/2)} \tag{3}$$

One of the important aspects of an explicit dynamic analysis is the time increment, which should be small enough to ensure a stable and converged analysis yet reasonably large to maintain an appropriate computational time. The stable time is determined based on the smallest dimension of the FE elements and the wave speed of the material [21]:

$$\Delta t_{stable} = L_e / c_d \tag{4}$$

in which L_e is the smallest dimension among all the elements in the FE model and c_d is the wave speed of the material.

Furthermore, the wave speed c_d can be estimated as follows [20]:

$$c_d = \sqrt{\frac{E}{\rho}} \tag{5}$$

in which E is the elastic modulus of the material; ρ is the density of the material.

The dynamic response of the pavement to the impulse LWD load is the resultant effect of the spectrum of stress waves that propagate in the pavement. In this study, the pavement FE model was restrained in the radial direction at the outer boundary. In FE modeling, it is likely that the stress wave impinges and reflects on the fixed outer boundary. However, during the LWD testing on

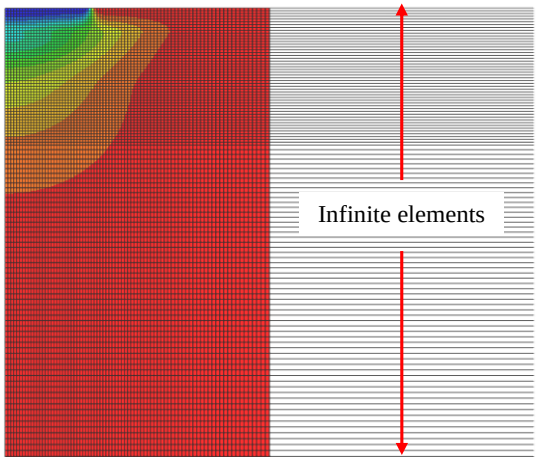

Fig. 5. Infinite Elements Assigned to the Outer Boundary of the Pavement FE Model.

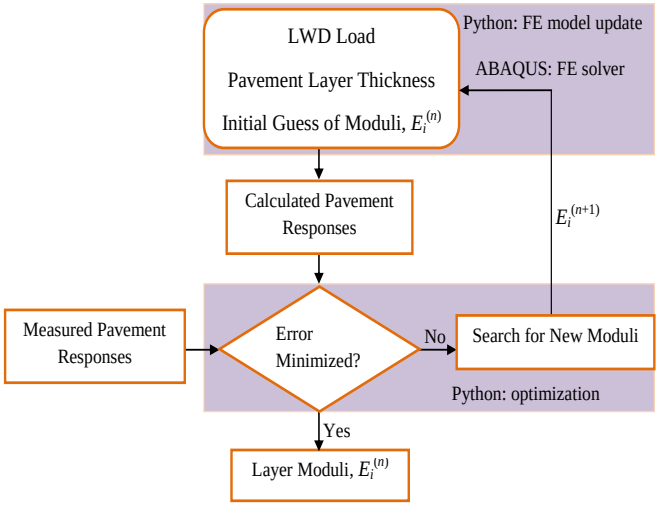

Fig. 6. Inverse Analysis Procedure for Evaluating the Pavement Layer Moduli.

Table 1. Boundary Constrains of the Pavement Layer Moduli

Pavement Layers	Elastic Modulus Ranges (MPa)
Asphalt Concrete	1000 - 3000
Base Course	50 – 200
Subgrade	5 - 100

pavement sections, the stress wave propagates beyond the distance between the load center and the FE outer boundary. Thus, it is necessary to address this phenomenon in order to have a simulation that more closely resembles the LWD testing.

Infinite elements are commonly used in FE modeling to simulate the far-field region, where the influence of the medium in the region is considered insignificant and is neglected. In this study, infinite elements were used as absorbing boundaries to transmit the impinging body waves [21]. The infinite elements are connected to the outer boundary of the finite elements in the FE model only, as shown in Fig. 5. No infinite elements were used at the bottom of the FE model because the stress wave energy dissipates along the travel path towards the bottom and the subsequent reflection at the bottom boundary was found to be minimal and negligible. It should be pointed out that the infinite elements adopted in this study do not simulate the geometries of the pavement test section.

Inverse Analysis

Inverse Analysis Procedures

Fig. 6 shows the inverse analysis procedure in which the optimization process is coupled with forward modeling/FE modeling to evaluate the pavement layer properties. Reasonable initial assumptions of material properties were made for the FE model before starting the inverse analysis. Traditional backcalculation typically uses only one set of initial inputs, while the inverse analysis procedure in this study starts with a population of initial inputs. The pavement responses were then calculated from the FE model with the initial material properties. The calculated pavement responses were compared to the measured responses until the difference between them was minimized to a satisfactory criteria.

The process of minimizing the difference between measured and calculated pavement responses was based on an optimization methodology, CMAES (Covariance Matrix Adaptation Evolution Strategy) developed by Hansen [22]. The optimization algorithm is written in an open-source programming language, Python [23] and communicates with the FE models created by using the ABAQUS® Python scripts.

Optimization Problem Formulation

Typically, an optimization problem includes the following three primary components:

(1) Optimization variables: these are usually the unknowns that need to be solved for, denoted as vector x. They are the pavement layer resilient moduli in this study.

(2) Constraints: the variables can be subjected to certain constraints in accordance with the physical meaning of the variables, denoted as $g(x) \leq 0$ and / or $h(x) = 0$. In this study, broad yet reasonable bounds of the individual variables were specified as presented in Table 1. The constraints among the variables were also applied to the optimization procedure: $E_{subgrade} \leq E_{base} \leq E_{asphalt}$. The optimization search space was narrowed by defining the bounds and constraints.

(3) Objective function: this is also called cost function, denoted as $f(x)$. The objective function is the root mean squared error (RMSE) between the measured pavement responses from the LWD load and the calculated pavement responses from the FE model: $f(x) = \sqrt{\frac{\sum_{i=1}^{n}(\delta_{mi} - \delta_{ci})^2}{(n-1)}}$ in which δ_{mi} is the measured value of the pavement response, such as surface and subgrade deflections; δ_{ci} is the calculated value of the pavement response from the FE model.

To define an optimization problem, a feasible set S is defined as a collection of all the points that satisfy the constraints $g(x) \leq 0$ and / or $h(x) = 0$. Then the procedure of optimization is essentially to find a vector $x^* \in S$ such that $f(x^*) \leq f(x)$ for all $x \in S$.

The Poisson's ratios were assumed and not considered

optimization variables because they do not influence the pavement responses within the range of typical values. Two measurements, surface deflection on the base layer and the subgrade deflection beneath the center of the LWD load, were used in the inverse analysis for the two-layer pavement structure (base-subgrade) to solve for two unknowns: E_{base} and $E_{subgrade}$. Three measurements—surface deflection on the asphalt layer and the deflection and vertical stress at the top of the subgrade—were used in the inverse analysis for the three-layer pavement structure (asphalt-base-subgrade) to solve for three unknowns: $E_{asphalt}$, E_{base}, and $E_{subgrade}$. The time histories of the surface deflection were used for the inverse analysis involving dynamic finite element modeling.

Optimization Method

The objective function in the problem formulation of this study is discontinuous and non-differentiable. Therefore, the traditional gradient-based optimization methods such as Newton's method and the Steepest Descent method are not applicable to this category of problem because they require information about the gradient of the objective function. The Covariance Matrix Adaptation Evolutionary Strategy (CMA-ES) optimization algorithm was adopted based on its well-recognized performance in solving difficult optimization problems [22] and its successful application in backcalculating pavement layer properties [24].

The CMAES belongs to the category of Evolutionary Algorithms (EAs), which are a class of stochastic search and optimization methods [25]. The algorithm is based on the principles of natural biological evolution and operates on a population of potential solutions, applying the principle of survival of the fittest to produce successively better approximations to a solution. The CMAES algorithm starts with a population of search points instead of a single point as most direct search methods do. An important and innovative feature of the CMAES algorithm is the definition of new search points. A new population is generated from a normal distribution expressed as [22]:

$$x_k^{(g+1)} \sim N\left(m^{(g)}, (\sigma^{(g)})^2\, C^{(g)}\right) \tag{7}$$

in which $k = 1, 2, \ldots. \lambda$ and λ is the size of population; $x_k^{(g+1)}$ is the k^{th} offspring / search points for generation g+1; $N\left(m^{(g)}, (\sigma^{(g)})^2\, C^{(g)}\right)$ represents a multivariate normal distribution in generation g; $m^{(g)}$ is the mean value of the search distribution at generation g; $\sigma^{(g)}$ is the overall standard deviation, step size at generation g; $C^{(g)}$ is the covariance matrix at generation g.

Each iteration or search step is accomplished by calculating values of $m^{(g)}$, $\sigma^{(g)}$,and $C^{(g)}$ for the next generation g+1. There are four parameters that are the key operators in CMAES: population size, adaptation, and change rates; population selection and recombination; step size control; and covariance matrix adaptation.

Verification of the Inverse Analysis Procedure using Synthetic Data

It is well-known that locating a global minimum is usually difficult, as well as the task of verifying the global minimum. In order to ensure that the inverse procedure and the optimization algorithm work for the specific problem in this study, the procedure was subjected to an examination before it was applied to solve the problem. A set of synthetic pavement response data were generated from the FE model with assumed pavement layer moduli, and the synthetic data were substituted for the measured values into the inverse procedure (Fig. 6). The inverse procedure was then carried out to find the "known" assumed pavement layer moduli.

The examination was conducted for both the two-layer system and three-layer system, as listed in Table 2. The difference between the backcalculated moduli values and the predefined layer moduli is negligible for both the two-layer and three-layer system, which indicates that the inverse analysis procedures and the optimization algorithm are capable of finding the global or best minimum and accurately estimating the pavement layer moduli. Figs. 7 and 8 display the iteration of the optimization procedures for the two-layer and three-layer pavement systems. It is worth pointing out that an inverse analysis converges when certain criteria are met, e.g. the objective function value is smaller than a prescribed value in this case. Fig. 8(b) shows that the objective function value becomes stable and approaches the prescribed value after about 240 iterations, although the asphalt layer modulus value appears to be transitioning in Fig. 8(a). In comparing Figs. 7 and 8, it took more iterations for the inverse analysis on the three-layer system to reach a satisfactory objective function value than for the two-layer system. The verification tests on the inverse analysis procedure showed the procedure is a viable process to find the pavement layer moduli.

Results of Inverse Analysis

Inverse analysis of the pavement layers' moduli were carried out based on instrumentation measurements and deflections measured on the surface. The inverse analysis procedure involved solving the FE models repeatedly until the convergence of the optimization procedures.

The pavement layers' elastic moduli were the only backcalculated material properties, while the other values for material properties in the FE model were assumed. The Poisson's ratios for the asphalt concrete, base layer, and subgrade were assumed to be: 0.3, 0.35, and 0.45, respectively [19]. Reasonable values were also assigned to

Table 2. Results of Inverse Analysis Using Synthetic Sata.

Runs	FE Models	Synthetic Measurements	Assumed Layer Moduli (MPa)	Backcalculated Moduli (MPa)
1	Two Layer Linear Static	Base Deflection Subgrade Deflection	Base: 20.0 Subgrade: 10.0	Base: 20.0 Subgrade: 10.0
2	Three Layer Linear Static	Asphalt Layer Deflection Subgrade Deflection Subgrade Vertical Stress	AC: 2000.0 Base: 20.0 Subgrade: 10.0	AC: 2007.0 Base: 19.9 Subgrade: 10.0

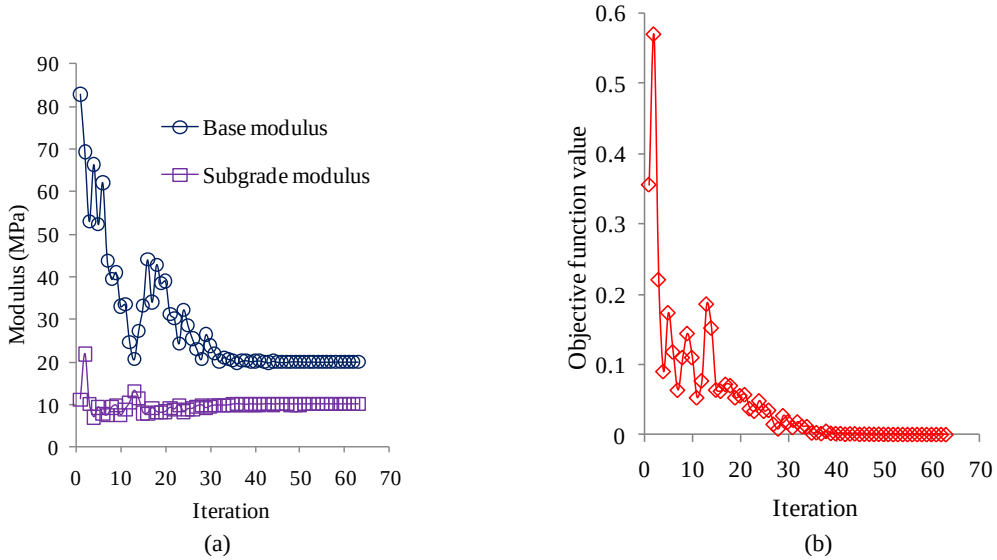

Fig. 7. Optimization Iteration for a Two-layer Pavement System: (a) Moduli of the Two Layers; (b) Objective Function Value.

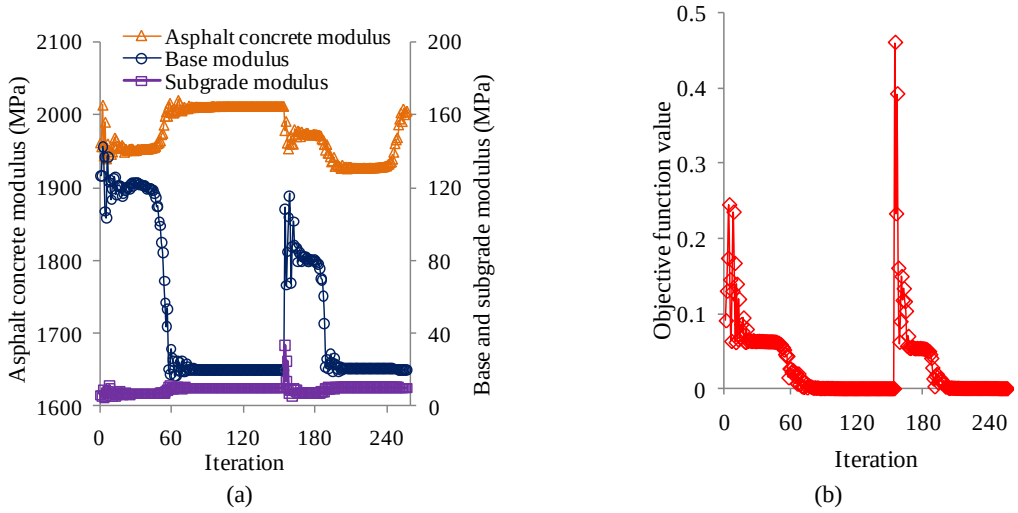

Fig. 8. Optimization Iteration for a Three-layer Pavement System: (a) Modulus of the Three Layers; (b) Objective Function Value.

damping ratios of the pavement materials during backcalculation based on dynamic analysis. The damping ratio for the soil subgrade is expected to be low, ranging from 0.01 to 0.03 [26]. In this study, the damping ratios for asphalt concrete, base, and soil subgrade were assumed to be: 0.06, 0.04, and 0.02. The Rayleigh damping coefficients – alpha and beta – were then estimated based on the relationship between the damping ratio, natural frequency of interests, and the damping coefficients. The values of alpha and beta for the asphalt concrete, base, and soil subgrade were: 47.2, 2.60×10^{-6}; 33.2, 1.95×10^{-6}; 11.1, 9.10×10^{-7}. According to Uzan [27], effects of damping ratios on backcalculating layers' properties are minimal. The mass density of asphalt concrete, base course, and subgrade soil were: 2247 kg/m^3, 2100 kg/m^3, and 1990 kg/m^3, respectively. A total of six sets of backcalculation were carried out. Listed in Table 3 are the results from the inverse analysis on pavement layer properties. Since LWD tests were conducted on the base layer and the asphalt layer along with the progress of construction, inverse analysis was conducted for both the two-layer and three-layer pavement structures. Static FE analysis was carried out when peak values of the LWD load were used in the FE model while the time-histories of LWD load were used for the dynamic FE analysis.

Inverse analysis based on static FE analysis was conducted using LWD tests on the base course layer and the asphalt layer built over Soil 1. Based on the results shown in Table 3, the backcalculated elastic moduli values for the base layer and subgrade are different between the two sets of static inverse analysis (Run 1 and Run 2). The base layer and subgrade exhibit higher stiffness resulting from the inverse analysis based on the LWD tests on the asphalt layer. The same observation was made for the pavement section built on Soil 2 (Run 4 and Run 5). One of the reasons is likely due to the further densification of the base layer and subgrade from the compaction of the asphalt layer. This also indicates that the addition of the asphalt layer may have changed the confining conditions of the unbound layers and consequently increased the moduli of the unbound base and subgrade layer.

In addition to the backcalculation conducted based on linear static analysis using peak values of measurements, the pavement layers'

Table 3. Results of Inverse Analysis Using Instrumentation Measurements.

Run	FE Model	Measured Pavement Response	Backcalculated Pavement Layer Moduli (MPa)
1	Two-layer Section with Soil 1 LWD Peak Stress: 64.6 kPa	Base deflection: 1.98 mm Subgrade Deflection: 1.66 mm	Base: 14.3 Subgrade: 4.8
2	Three-layer Section with Soil 1 LWD Peak Stress: 129.6 kPa	Asphalt Deflection: 0.82 mm Subgrade Deflection: 0.59 mm Subgrade Vertical Stress: 12.6 kPa	AC: 1684.0 Base: 43.5 Subgrade:12.2
3	Three-layer Section with Soil 1 LWD Time-history Load	Time-history Data of Asphalt Layer Deflection at the Center of Load	AC: 1401.2 Base: 37.5 Subgrade:15.1
4	Two-layer Section with Soil 2 LWD Peak Stress: 66.1 kPa	Base Deflection: 1.99 mm Subgrade Deflection: 1.80 mm	Base: 12.0 Subgrade: 3.1
5	Three-layer Section with Soil 2 LWD Peak Stress: 130.0 kPa	Asphalt Deflection: 1.04 mm Subgrade Deflection: 0.80 mm Subgrade Vertical Stress: 11.2 kPa	AC: 1705.1 Base: 27.8 Subgrade: 9.0
6	Three-layer Section with Soil 2 LWD Time-history Load	Time-history Data of Asphalt Layer Deflection at the Center of Load	AC: 1480.0 Base: 23.9 Subgrade: 12.8

moduli were backcalculated through linear dynamic models using measured time-histories of the LWD load and corresponding pavement deflection. Fig. 4 shows the time histories of the measured load, measured deflection, and modeled deflection. The modeled deflection matches well with the measured deflection. It is noted that the backcalculated moduli of the asphalt layer and base layer are lower than those from backcalculation based on static analysis for both sets of pavement sections. The backcalculated subgrade modulus in the pavement test section with Soil 2 is lower than that in pavement test section with Soil 1, which is consistent with the fact that the subgrade with Soil 2 was a weaker subgrade with lower CBR.

The backcalculated asphalt layer moduli vary between 1401 MPa and 1705 MPa (Table 3). While the values of the asphalt moduli are not completely out of range, they are near the lower boundary of anticipated asphalt moduli. This is likely attributed to the inadequate compaction carried out by using a small vibratory plate compactor that probably does not generate the needed compaction energy. Measurements of air voids of the asphalt layer by a pavement quality indicator (PQI) showed a high air void content ranging from 7.3% to 12.0% with an average value of 9.9%. As a result, the density and modulus of the asphalt concrete is low in this study. It should be pointed out that the tests were conducted in an indoor lab, and the asphalt concrete temperatures were recorded throughout the tests using a K-type thermocouple. The recorded temperature varies from 24.2℃ to 27.0℃ with an average value of 25.6℃, indicating that the ambient temperature during the tests does not play a role in resulting in the low stiffness of the asphalt concrete layer.

Compared to the anticipated values listed in Table 1, the backcalculated moduli of the base layer are relatively low. It should be pointed out that the range of the modulus value given in Table 1 does not guarantee that the backcalculated value falls in the range. Instead, it generates the initial population of layer moduli within the range, i.e. the starting points of the search for optimal values. The low modulus value of the base layer was most likely due to inadequate compaction of the aggregate base during construction, which is consistent with the fact that the aggregate base was constructed over a soft soil subgrade with a CBR value from 1.5 to 2.0 and unable to be fully compacted. Furthermore, the LWD loading level in this study is lower than the standard wheel axle load and the FWD load. Given the stress-dependent nature of the unbound materials, a higher loading level may result in a higher modulus value. A nonlinear resilient modulus model (e.g. the k-θ model, Uzan-Witczak model, and MEPDG universal resilient model) may be adopted in the forward modeling for the base aggregate to account for its stress-dependent behavior.

Summary and Conclusions

This study demonstrates the use of instrumentation measurements in a generalized inverse analysis procedure. The inverse analysis procedure involves a population-based optimization algorithm coupled with FE models. Two sets of pavement sections were constructed such that the sections had the same dimensions and same pavement materials except for the subgrade soil types and conditions. The subgrade layers were constructed at CBR= 2 (Soil 1) and CBR= 1.5 (Soil 2). The two flexible pavement test sections were instrumented with LVDTs to measure soil subgrade deflections and pressure cell to measure the vertical stress. A lightweight deflectometer (LWD) was used to test the structural properties of the two flexible pavement test sections. Pavement surface deflection and subgrade deflection were recorded in response to the LWD impulse load. The measurements were then used in an inverse analysis procedure to backcalculate the pavement layers' moduli.

Results generated from the inverse analysis conducted on the two sets of flexible pavement test sections show pavement layer moduli that are consistent with the experimental measurements. The primary findings from this study are summarized as follows:

- An inverse analysis procedure was developed and its effectiveness of backcalculating flexible pavement layer

properties was demonstrated.

- The generic inverse procedure adopted in this study showed that it is possible to backcalculate pavement layer properties based on any known input signals (LWD load in this case) and any properly measured output signals (pavement responses from embedded instrumentation and surface deflections in this case) of the pavement system. Furthermore, the procedure showed the attribute of broad applicability by using commercially-available and general-purpose numerical modeling packages coupled with well-developed open source of optimization algorithms.
- Although the backcalculated modulus values of the asphalt and base layers were consistent through the two sets of tests, they both are relatively low mainly due to the inadequate compaction during the construction. Furthermore, compared to the FWD load and a standard full-scale axle load, the LWD loading level is lower and may play a role in resulting in a low backcalculated modulus for the aggregate base layer. A nonlinear resilient modulus model would better characterize the stress-dependent behavior of the unbound aggregate layer.
- Given the trend that the application of pavement instrumentation is continuously growing, the inverse analysis procedure can be potentially extended to evaluate and monitor the layer moduli of instrumented in-service pavements with decreased interruption of traffic. The difficulty for practical implementations of this inverse analysis procedure lies in its FE forward modeling, particularly the dynamic FE modeling which requires a large amount of computational time and resources. Substituting the FE model with a surrogate such as a Neural Network model would significantly increase the efficiency of the inverse analysis procedure.

Acknowledgements

The authors would like to thank the Pennsylvania Department of Transportation for financially supporting this study. The authors would also like to thank Mr. Dan Fura for his assistance with the experimental work.

References

1. Brown, S.F. (1977). State-of-the-Art Report on Field Instrumentation for Pavement Experiments. *Transportation Research Record*, No. 640, pp. 13-28.
2. Ullidtz, P. and Larsen, E.H.J. (1989). State-of-the-Art Stress, Strain, and Deflection Measurements. *Proceedings of the First International Symposium on the State of the Art of Pavement Response Monitoring Systems for Roads and Airports*, Lebanon, NH, USA.
3. Tabatabaee, N., Al-Qadi, I.L., and Sebaaly, P.E. (1992). Field Evaluation of Pavement Instrumentation Methods. *Journal of Testing and Evaluation*, 20(2), pp. 144-151.
4. Baker, H.B., Buth, M.R., and Van Deusen, D.A. (1994). Minnesota Road Research Project: Load Response Instrumentation Installation and Testing Procedures. *Final Report No. MN/PR-94/01*. Minnesota Department of Transportation, St. Paul, Minnesota, USA.
5. Brandon, T.L., Al-Qadi, I.L., Lacina, B.A. (1996). Construction and Instrumentation of Geosynthetically Stabilized Secondary Road Test Sections. *Transportation Research Record*, No. 1534, pp. 50-57.
6. Timm, D.H., Priest, A.L., and McEwen, T.V. (2004). Design and Instrumentation of the Structural Pavement Experiment at the NCAT Test Track, NCAT Report 04-01. National Center for Asphalt Technology, Auburn, AL, USA.
7. AASHTO (2008). Mechanistic-Empirical Pavement Design Guide, Interim Edition: A Manual of Practice. AASHTO, Washington, DC, USA.
8. NCHRP (2004). NCHRP Project 1-37A Design Guide, Mechanistic-Empirical Design of New and Rehabilitated Pavement Structures. Final Report, NCHRP Study 1-37A, National Cooperative Highway Research Program (NCHRP), Transportation Research Board of the National Academies, Washington, DC, USA.
9. Hornyak, N.J., Crovetti, J.A., Newman, D.E., and Shabelski, J.P. (2007). Perpetual Pavement Instrumentation for the Marquette Interchange Project-Phase I. *Report No. WHRP 07-11*. Wisconsin Department of Transportation, Madison, Wisconsin, USA.
10. Sargand, S., Figueroa, J. L., and Romanello, M. (2008). Instrumentation of the WAY-30 Test Pavements, Final Report FHWA/OH-2008/7 , Ohio Department of Transportation, Office of Research and Development, Columbus, OH 43223.
11. Timm, D. (2009) I-35 Pavement Instrumentation Phase II, *FHWA-OK-09-04*, Oklahoma Department of Transportation, Planning and Research Division, Oklahoma City, OK, USA.
12. Lajnef, N., Rhimi, M., Chatti, K., and Mhamdi, L. (2011). Toward an Integrated Smart Sensing System and Data Interpretation Techniques for Pavement Fatigue Monitoring. *Computer-Aided Civil and Infrastructure Engineering*, 26, pp. 513-523.
13. Lian, K. (2010). Developing Embedded Wireless Strain/Stress/Temperature Sensor Platform for Highway Applications. Final Report for NCHRP IDEA Project 129, TRB, National Research Council, Washington, DC, USA.
14. Lytton, R. L. (1989). Backcalculation of Pavement Layer Properties." Nondestructive Testing of Pavements and Backcalculation of Moduli, A.J. Bush III and G.Y. Baladi (eds.), *STP 1026*, American Society for Testing and Materials, Philadelphia, PA, USA, pp. 7–38.
15. Irwin, L. (2002). Backcalculation: An overview and perspective. *Proceedings of Workshop 3, 6th International Conference on Bearing Capacity of Roads, Railways and Airfields*, Lisbon, Portugal.
16. Santamarina, J.C., and Fratta, D. (2005). *Discrete Signals and Inverse Problems, an Introduction for Engineers and Scientists*, John Wiley & Sons, West Sussex, UK.
17. Wimsatt, A.J., Scullion, T., Fernando, E., Hurlebaus, S., and Lytton, R. (2009). A Plan for Developing High-Speed Nondestructive Testing Procedures for Both Design Evaluation and Construction Inspection. SHRP 2 Report S2-R06-RW, Strategic Highway Research Program, Transportation Research Board, Washington, DC, USA.
18. Palomino, A.M., Tang, X., and Stoffels, S.M. (2010). Determination of Structural Benefits of PennDOT-Approved

Geogrids in Pavement Design. Report No. *FHWA-PA-2010-012-PSU 018*, Final Report Submitted to the Pennsylvania Department of Transportation, Harrisburg, PA, USA.

19. Huang, Y.H. (1993). *Pavement Analysis and Design*, Pearson Prentice Hall, Upper Saddle River, NJ, USA.
20. Richart, F.E., Woods, R.D., and Hall, J.R. (1970). *Vibrations of Soils and Foundations*, Prentice-Hall, Englewood Cliffs, NJ, USA.
21. SIMULIA (2009). Abaqus Analysis User's Manual, Abaqus version 6.9, Providence, RI, USA.
22. Hansen, N. (2006). The CMA Evolution Strategy: A Comparing Review. In *Towards a New Evolutionary Computation. Advances in Estimation of Distribution Algorithms*, J.A. Lozano, P. Larrañga, I. Inza and E. Bengoetxea (eds.), Springer Berlin Heidelberg, Berlin, Germany, pp. 75-102..
23. Hansen, N. (2010). Personal Communications.
24. Gopalakrishnan, K. and Manik, A. (2010). Co-Variance Matrix Adaption Evolution Strategy for Pavement Backcalculation. *Construction and Building Materials*, 24, pp. 2177-2178.
25. Beyer, H.G. and Schwefel, H.P. (2002). Evolution Strategies – A Comprehensive Introduction. *Natural Computing*, Vol. 1, pp.3-52.
26. Chang, D.W., Kang, Y.V., Roesset, J.M., and Stokoe, K.H. (1991). Effect of Depth of Bedrock on Deflection Basins Obtained with Dynaflect and FWD Tests. *Transportation Research Record*, No. 1355, pp. 8-17.
27. Uzan, J. (1994). Dynamic Linear Backcalculation of Pavement Material Properties. *Journal of Transportation Engineering*, 120(1), pp. 109-126.